A neural-network approach for quantitative precipitation estimation using an operational polarimetric C-band radar in complex terrain scenarios

Gianfranco Vulpiani

Gianfranco Vulpiani[1]

[1]*Department of Civil Protection, via Vitorchiano 2, Rome, Italy*

(Dated: 26th August 2014)

1. Introduction

Weather radar observations provide valuable information for the real-time monitoring and nowcasting of severe precipitation phenomena. However, it is known that any quantitative use of radar measurements is heavily conditioned by several uncertainty sources (e.g., Wilson and Brandes (1979)). Among others, it is worth recalling effects related to orography (e.g., ground clutter, partial or total beam blocking), range distance (e.g., precipitation overshooting, beam broadening, non-uniform beam filling), electromagnetic processes (e.g., attenuation, resonance), precipitation characteristics (e.g., space-time variability of raindrop size distribution (RSD), contamination by frozen and/or melting hydrometeors), etc. Notwithstanding, significant technological (hardware, software) and scientific progresses have been achieved in the last decades, bringing to a noticeable progress in quantitative precipitation estimation, as remarked by Krajewski et al. (2010).

In this contest, dual-polarization capability played a crucial role improving the identification of non-meteorological echoes Gourley et al. (2007), compensating rain path attenuation (e.g., Bringi et al. (1990, 2001); Carey et al. (2000); Testud et al. (2000)), classifying hydrometeors (e.g., Marzano et al. (2007, 2008); Ryzhkov et al. (2005b); Straka et al. (2000)), reducing the consequences of drop size distribution variability on the retrieval process Bringi et al. (2004); Gorgucci et al. (2002, 2000).

Nowadays, the maturity achieved by polarimetric techniques persuaded many weather services, especially in Europe, to invest on this technology. Indeed, within the operational community, an attractive feature of dual-polarization technology is the capability to monitor the system functioning revealing calibration and interference issues, e.g., Figueras i Ventura et al. (2012); Gourley et al. (2006).

The benefit deriving by the use of polarimetry for operational quantitative precipitation estimation (QPE) in mountainous areas was demonstrated in Vulpiani et al. (2012). In that work, the Authors found that algorithms employing specific differential phase (K_{dp}), properly processed through a new iterative technique, generally outperformed those using reflectivity. The key role played by K_{dp} was also emphasized in real-time operational conditions by Figueras i Ventura et al. (2012), where, due to the difficulty to achieve the appropriate calibration accuracy, the use of Z_{dr} for QPE purposes was considered “unsafe”.

These findings are mainly related to the well known insensitivity of K_{dp} to partial beam blocking and attenuation. Nevertheless, as shown in Vulpiani et al. (2012), $R(K_{dp})$ algorithms might be sensitive to wet or dry ice contamination, especially at far ranges during winter storms, and to RSD variability.

In the light of the aforementioned results, the present study is aimed at integrating the aforementioned work (i.e., Vulpiani et al. (2012)) by: 1) tuning the K_{dp}-retrieval technique, 2) compensating the effects of the vertical variability on K_{dp} by ground projecting the K_{dp} fields retrieved aloft, 3) reducing the effects of RSD variability adopting a multi-parameter (i.e., Z and K_{dp}) algorithm for rainfall estimation based on neural networks (NN). Indeed, in Vulpiani et al. (2009), it was found that the proposed Neural-Network inversion techniques, trained on a generic simulated data set, have generally outperformed the considered climatologically-tuned parametric algorithms.

For these purposes, a dozen of events observed by a C-band polarimetric system located in the Abruzzo region in central Italy and managed by the Italian Department of Civil Protection have been analyzed. The manuscript is organized as follows: the applied pre-processing chain is summarized in Sect. 2, the proposed NN algorithm is described in Sect. 3, whereas the comparative performance analysis is discussed in Sect. 4.

2. Data processing

The radar processing chain here adopted is briefly described in this section. It has been conceived to deal with contamination by non-weather resturns (clutter), Partial Beam Blocking (PBB), beam broadening at increasing distances, vertical variability of precipitation, inversion of radar observables into rainfall rate.

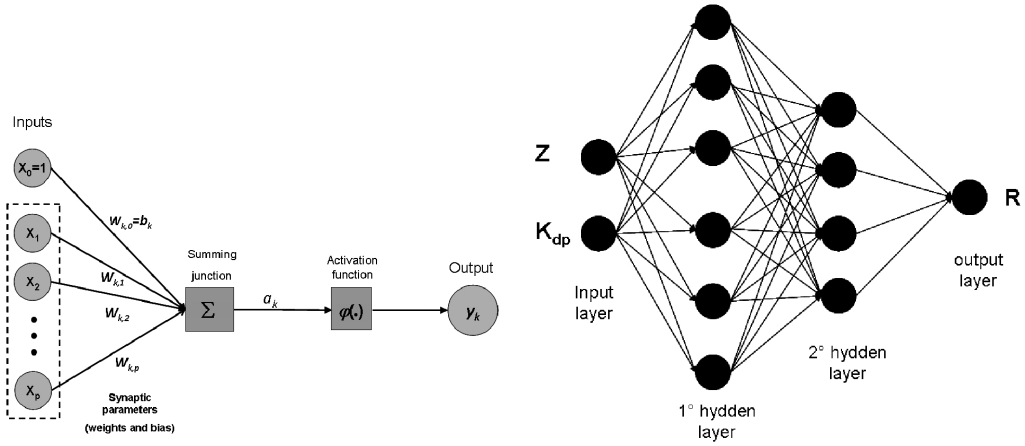

Figure 1: Schematic representation of the non-linear neuron model (upper panel) and architecture of the neural-network algorithm conceived for polarimetric radar rainfall estimation (lower panel).

The data processing begins with the identification and compensation for non-meteorological echoes and partial beam blockage effects. Second, K_{dp} is derived from the filtered Φ_{dp} (Vulpiani et al., 2012) and used in the rain path attenuation correction module based on the procedure proposed by Vulpiani et al. (2008). The mean Vertical Profile of Reflectivity (VPR) is then retrieved in real time and applied to the considered reflectivity-based radar products. Next, the mean Vertical Profile of K_{dp} (VPK), computed on a daily basis, is applied to the estimated K_{dp} fields. Finally, rain rates are computed either using power laws employing Z and K_{dp}, separately, or a neural network ingesting both.

3. Rainfall estimation

3.1. Parametric techniques

A standard Z-R relationship (Marshall and Palmer (1948)) is applied to the considered reflectivity product. Regarding the K_{dp}-based rain rate algorithm, we have considered a general expression of the form $R = a|K_{dp}|^b sign(K_{dp})$ as suggested by Ryzhkov et al. (2005a). Despite this formula provides unrealistic negative rain rates for negative Kdp values, it is adopted in order to compensate the noise effects on the retrieved Kdp (i.e., slightly positive and negative rain rates tend to cancel each other when computing the cumulated rainfall). Considering the power-law parameters (a, b) derived by Bringi and Chandrasekar (2001) and Bringi et al. (2011) the tested algorithms, respectively denoted as R_{BC01} and R_{BR11}, are:

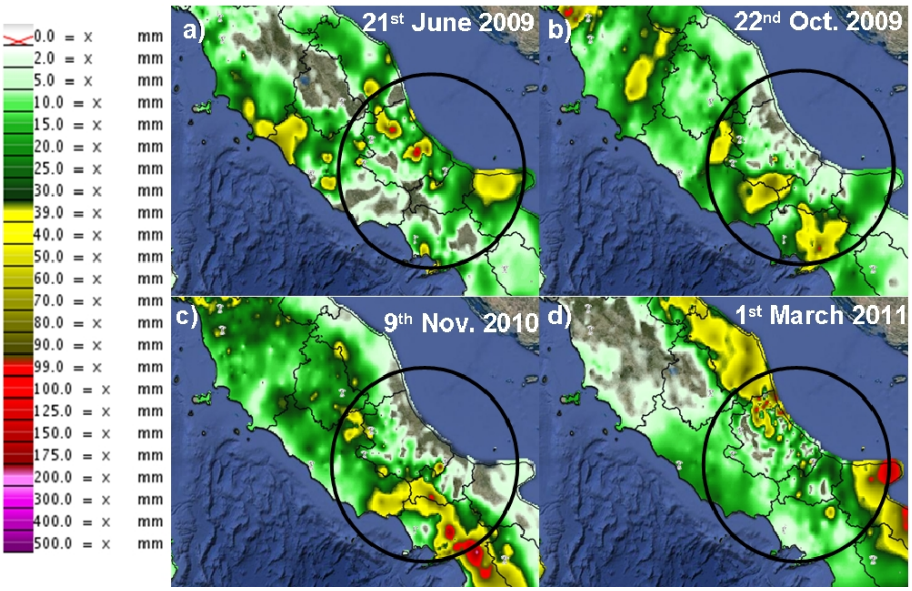

Figure 2: 24-h cumulated rainfall as observed by the rain gauge network in central Italy. Panels a)-d) refer to the events observed on 2009/06/21, 2009/10/22, 2010/11/09 and 2011/03/01.

$$R_{BC01} = 129\left(\frac{|K_{dp}|}{f}\right)^{0.85} sign(K_{dp}) \tag{3.1}$$

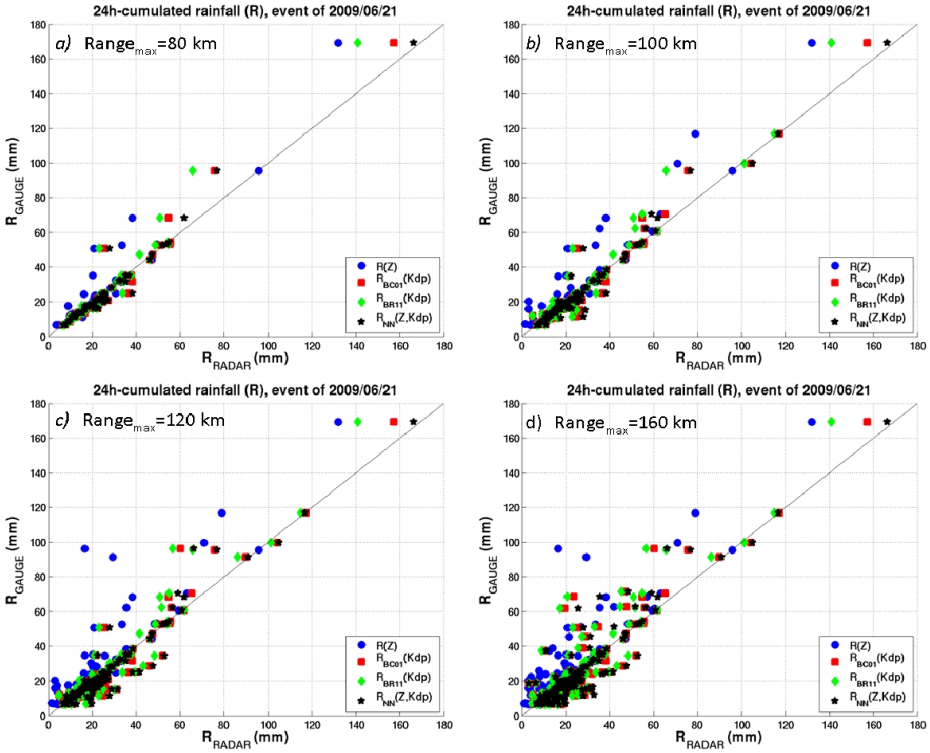

Figure 3: Comparison of 24-h cumulated radar rainfall estimates and gauge observations at increasing range domain for the event observed on 21 June 2009.

$$R_{BC01} = 24.68|K_{dp}|^{0.81} sign(K_{dp}) \tag{3.2}$$

where f is the radar frequency expressed in GHz. The relationships (3.1) and (3.2) have been applied to the lowest beam map of K_{dp} with and without ground projection by means of the retrieved *VPK*.

3.2. Neural Network retrieval technique

Generally speaking, an artificial neural network can be considered as a non-linear parameterized mapping from an input x to an output $y = NN(x; w, M)$, where w is the vector of parameters (weights and biases) relating the input x to the output y, while the functional form of the mapping (i.e., the architecture of the net) is denoted as M.

As depicted in Fig. **??**, the basic processing unit, the neuron, is modeled as: 1) a set of synapses, each of which is characterized by a weight, 2) an adder for summing the input signals, weighted by the respective synapses of the neuron, 3) an activation function (φ) for limiting the amplitude of the output of a neuron. In mathematical terms, a given neuron output y_k can be written as

$$y_k = \varphi(a_k) \tag{3.3}$$

with

$$a_k = \sum_{k=0}^{p} w_{k,j} x_j = \sum_{k=1}^{p} (w_{k,j} x_j + b_k) \tag{3.4}$$

where x_j is the input to the *j*-th synapse, $w_{k,j}$ the synaptic weight, $b_k = w_{k,0} x_0$ (with $x_0 = 1$) the bias and φ the activation function. (3.4) can be written in matrix form as

$$a_k = w_k^T x \tag{3.5}$$

The multi-layer perceptron architecture (MLP), considered here, is a mapping model composed of several layers of parallel processors. It has been theoretically proven that one-hidden layer MLP networks may represent any non-linear continuous function Haykin (1998), while a two-hidden layer MLP may approximate any function to any degree of non-linearity taking also into account discontinuities (Sontag (1992)). A crucial step for setting up the neural network is the training, or learning process. During this step the synaptic weights of the network are modified by applying a set of labeled training samples or task samples.

For a MLP network, (3.5) can be generalized for the *i*-th layer as

$$Y^{(i)} = \varphi^{(i)}(A^{(i)}) \tag{3.6}$$

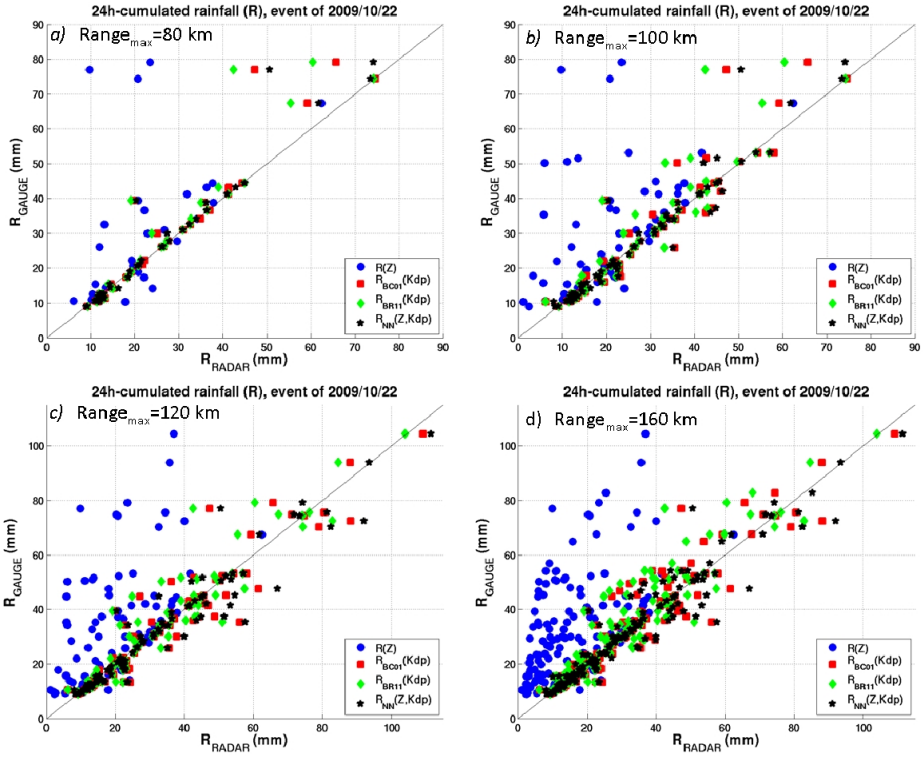

Figure 4: As in Fig. 3 but relatively to the event observed on 2009/10/22.

Node	b_k	$w_{k,1}$	$w_{k,2}$
k=1	-0.0745	-0.2073	0.5410
k=2	0.7801	-1.1215	0.4841
k=3	-0.4264	0.4924	0.2961
k=4	0.2563	-0.4140	-0.1930
k=5	-0.0151	0.5420	0.6836
k=6	1.0174	0.2675	-0.1798

Table 1: Synaptic parameters connecting the input array (i.e., $x_1 = Z$, $x_2 = K_{dp}$), first normalized then transformed through φ, to the 1st hydden layer.

with $Y = [y_1\, y_2\, ...y_N]$, and

$$A = W \cdot X = \begin{bmatrix} b_1 & w_{1,1} & ... & w_{1,p} \\ b_2 & w_{2,1} & ... & w_{2,p} \\ \vdots & \vdots & \ddots & \vdots \\ b_n & w_{n,1} & ... & w_{n,p} \end{bmatrix} \begin{bmatrix} 1 \\ x_1 \\ \vdots \\ x_p \end{bmatrix} \tag{3.7}$$

where p is the number of input to the i-th layer composed by n nodes.

In this work, a neural network rainfall algorithm employing Z and K_{dp} [denoted as $R_{NN}(Z, K_{dp})$] has been set up applying, as in Vulpiani et al. (2009), a regularization technique during training to get the desired generalization capability. The designed neural-network architecture, composed by 2 hydden layers with respectively 6 and 4 nodes, is depicted in Fig. 2.

The synaptic parameters W connecting respectively the input to the 1st layer, the 1st and 2nd hydden layers, the 2nd to the output layers are reported on Tabs. 1 - 4. A tan-sigmoid activation function [(e.g., $\varphi(x) = 2/(1 + exp(-2x)) - 1$] is generally adopted except for the output layer ($i = 4$) where a linear transformation function (e.g., $\varphi(x) = x$) is applied.

It is worth specifyng that the input nodes at the first layer are typically normalized, whereas the output nodes are de-normalized after applying the activation function. In this work the input vector is normalized with respect to the mean and

Node	b_k	$w_{k,1}$	$w_{k,2}$	$w_{k,3}$	$w_{k,4}$	$w_{k,5}$	$w_{k,6}$
k=1	-0.4847	-0.1609	0.2012	-0.3379	0.0788	-0.7145	0.0822
k=2	0.0251	-0.4901	-0.2438	-0.0150	0.0921	-0.0566	-0.1943
k=3	-0.1040	0.4216	0.9390	-0.0223	-0.0187	0.7099	-0.4829
k=4	-0.532	0.1862	1.0097	0.2245	-0.1332	0.5568	0.0694

Table 2: Synaptic parameters connecting the output of the 1st hydden layer to the 2nd hydden layer.

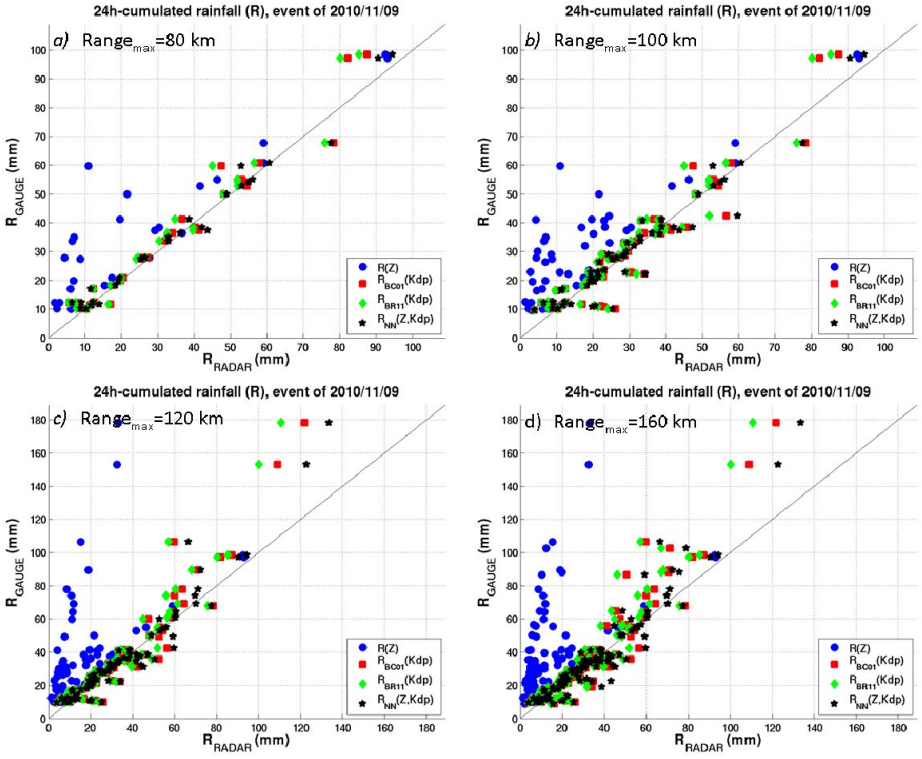

Figure 5: As in Fig. 3 but relatively to the event observed on 2010/11/09.

	$Z(dBZ)$	$K_{dp}(deg\,km^{-1})$	$R(mm\,h^{-1})$
$mean$	38.7	0.8	22.0
σ	6.0	1.3	32.0

Table 3: Normalization parameters adopted for the proposed neural network rainfall estimation algorithm.

standard deviation of the training data set. See Tab. 3 for the normalization parameters.

Overall, the procedure can be summarized in the following steps:

i. the input array $X^{(0)} = [Z\, K_{dp}]$, normalized and then transformed through the activation function, represents the input to the second layer (first hidden layer) and is denoted as $x^{(1)}$;

ii. the output of the second layer is obtained through (3.7) using the connection parameters reported on Tab. 1 and applying the activation function, i.e., $Y^{(1)} = \varphi(W^{(1)}X^{(1)})$;

iii. similarly to step $ii.$, the output of the 3rd layer (2nd hidden layer) is obtained as $Y^{(2)} = \varphi(W^{(2)}X^{(2)})$, where $X^{(2)} = Y^{(1)}$;

iv. finally, the rainfall rate is obtained by de-normalizing the output of the 4th layer, i.e., $Y^{(3)} = \varphi(W^{(3)}X^{(3)})$, with $X^{(3)} = Y^{(2)}$;

Regarding step $i.$, it is important to specify that the input fields of reflectivity and specific differential phase have been obtained considering the corresponding lowest beam maps, both projected at ground through the estimated VPR and VPK, respectively.

4. Results

Several rainfall episodes observed by the polarimetric C-band radar located in Tufillo (Chieti,Italy) are considered in the present work. A special focus is dedicated to the analysis of four of them having different microphysical and observational characteristics: 21 June 2009, 22 October 2009, 9 November 2010, 1 March 2011. Figure 2 shows the 24-h cumulated precipiation observed by the available rain gauge network as interpolated through a Kriging-like approach named GRISO developed by CIMA Research Foundation (www.cimafoundation.org). The first considered precipitaion episode was a convective event with generally moderate rainfall amount, except for some localized peaks relatively close to the radar site. The second event was a tipically stratiform event generally characterized by moderate rainfall amount at far range from the radar. The event observed on the 9th of november 2010 was a stratiform event with moderate-to-high registred precipitation amount at medium to far ranges. Finally, the 1st of March 2011 was a spatially-heterogeneous precipitation event with winter convective circunstances determining spread areas of moderate-to-high rainfall amount (e.g., see the south-eastearn part of the radar domain)

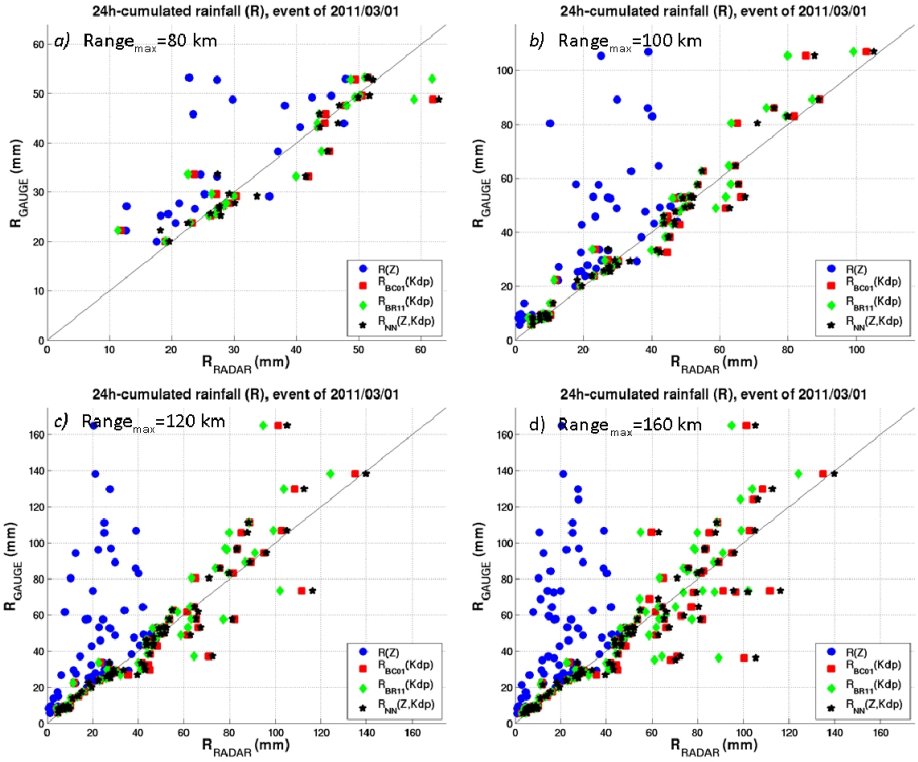

Figure 6: As in Fig. 3 but relatively to the event observed on 2011/03/01.

Node	b_k	$w_{k,1}$	$w_{k,2}$	$w_{k,3}$	$w_{k,4}$
k=1	0.4657	-1.0147	-0.5227	1.4739	1.4289

Table 4: Synaptic parameters connecting the output of the 2nd hydden layer to the output.

and localized peaks of precipitation sporadically contaminated by melting snow. Figures 3-6 show the comparison between gauge observations and radar estimates at differents range distances for every considered rainfall algorithm. Regarding the first event it is possible to note that all the applied techniques, including the Z-R relationship, provide relatively good performance with a modest sensitivity with respect to range distance. This might be related to the fact that most of the precipitation fell within the azimuthal sector with relatively good visibility, so that reflectivity was not perturbed that much by the beam blocking. Furthermore, the altitude-related uncertainty sources were reasonably negligible due to the the relatively high freezing layer height. The situation is considerably different for the other considered events. Indeed, a clear range-related accuracy can be noticed mainly for the Z-R algorithm, whereas the polarimetric relationships and especially the Neural Network approach provided better performance in terms of mean error, error standard deviation and mean ratio bias.

5. Conclusions

In this work, most ofthe error sources affecting the estimation process are dealt taking advantage by the dualâpolarization capability of the considered operational Câband system belonging to the Italian radar network. Indeed,precipitation is estimated after compensating for ground-clutter, partial beam blocking, attenuation and vertical variability. Furthermore, differential phase is processed through an iterative moving-window finite-difference scheme allowing to keep under control the K_{dp} standard deviation and easily remove any system offset. A special focus is dedicated to the development and testing of a new neuralânetwork technique employing reflectivity and specific differential phase. The comparative performance analysis, accomplished on some rainfall events occurred in central Italy, highlights the flexibility and efficiency of the suggested methodology confirming the previous findings (Vulpiani et al., 2009). The arcane, often accompanying neural networks applications, is unraveled providing details for the operational implementation of the proposed technique. Future works will be devoted to a long-period assessment to verify the operational utility of the proposed approach.

References

Bringi, V. N. and V. Chandrasekar, 2001: *Polarimetric doppler weather radar*. Cambridge University Press, 636 pp.

Bringi, V. N., V. Chandrasekar, N. Balakrishnan, and D. S. Zrnić, 1990: An examination of propagation effects in rainfall on radar measurements at microwave frequencies. *J. Atmos. Oceanic Technol.*, **7**, 829–840.

Bringi, V. N., T. D. Keenan, and V. Chandrasekar, 2001: Correcting C-band radar reflectivity and differential refelctivity data for rain attenuation: a self-consistent method with constraints. *IEEE Trans. Geosci. Rem. Sens.*, **39**, 1906–1915.

Bringi, V. N., M. A. Rico-Ramirez, and M. Thurai, 2011: Rainfall estimationwith an operational polarimetric C-band radar in the united kingdom: comparison with gauge network and error analysis. *J. Hydrometeor.*, **12**, 935–954.

Bringi, V. N., T. Tang, and V. Chandrasekar, 2004: Evaluation of a new polarimetrically based Z-R relation. *J. Atmos. Oceanic Technol.*, **21**, 612–623.

Carey, L. D., S. A. Rutledge, and D. A. Ahijevych, 2000: Correcting propagation effects in C-band polarimetric radar observations of tropical convection using differential propagation phase. *J. Appl. Meteor.*, **39**, 1405–1433.

Figueras i Ventura, J., A. Boumahmoud, B. Fradon, P. Dupuy, and P. Tabary, 2012: Long-term monitoring of french polarimetric radar data quality and evaluation of several polarimetric quantitative precipitation estimators in ideal conditions for operational implementation at C-band. *Q. J. R. Meteorol. Soc.*, doi:10.1002/qj.1934.

Gorgucci, E., V. Chandrasekar, V. N. Bringi, and G. Scarchilli, 2002: Estimation of raindrop size distribution parameters from polarimetric radar measurements. *J. Atmos. Sci.*, **59**, 2373–2384.

Gorgucci, E., G. Scarchilli, V. Chandrasekar, and V. N. Bringi, 2000: Measurement of mean raindrop shape from polarimetric radar observations. *J. Atmos. Oceanic Technol.*, **57**, 3406–3413.

Gourley, J. J., P. Tabary, and J. Parent du Chatelet, 2006: Data quality of the Meteo-France C-band polarimetric radar. *J. Atmos. Oceanic Technol.*, **23**, 1340–1356.

Gourley, J. J., P. Tabary, and J. Parent du Chatelet, 2007: A fuzzy logic algorithm for the separation of precipitating from non-precipitating echoes using polarimetric radar observations. *J. Atmos. Oceanic Technol.*, **24**, 1439–1451.

Haykin, S., 1998: *Neural networks: a comprehensive foundation*. Prentice Hall; 2 edition, 842 pp.

Krajewski, W. F., G. Villarini, and J. A. Smith, 2010: Radar-rainfall uncertainties. *Bull. Amer. Meteor. Soc.*, **91**, 87–94.

Marshall, J. S. and W. M. Palmer, 1948: The distribution of raindrops with size. *J. Meteor.*, **5**, 165–166.

Marzano, F. S., D. Scaranari, and G. Vulpiani, 2007: Supervised fuzzy-logic classification of hydrometeors using C-band weather radars. *IEEE Trans. Geosci. Rem. Sens.*, **45**, 3784–3799.

Marzano, F. S., D. Scaranari, G. Vulpiani, and M. Montopoli, 2008: Supervised classification and estimation of hydrometeors using C-band dual-polarized radars: a bayesian approach. *IEEE Trans. Geosci. Rem. Sens.*, **46**, 85–98.

Ryzhkov, A. V., S. Giangrande, and T. J. Schuur, 2005a: Rainfall estimation with a polarimetric prototype of WSR-88D. *J. Appl. Meteor.*, **44**, 502–515.

Ryzhkov, A. V., T. J. Schuur, D. W. Burgess, P. L. Heinselman, S. E. Giangrande, and D. S. Zrnic, 2005b: The joint polarization experiment: Polarimetric rainfall measurements and hydrometeor classification. *Bull. Amer. Meteor. Soc.*, **86**, 809–824.

Sontag, E., 1992: Feedback stabilization using two-hidden-layer nets. *IEEE Trans. Neural Networks*, **3**, 981–990.

Straka, J. M., D. S. Zrnić, and A. Ryzhkov, 2000: Bulk hydrometeor classification and quantification using polarimetric radar data: synthesis of relations. *J. Appl. Met.*, **39**, 1341–1372.

Testud, J., E. L. Bouar, E. Obligis, , and M. Ali-Mehenni, 2000: The rain profiling algorithm applied to polarimetric weather radar. *J. Atmos. Oceanic Technol.*, **17**, 332–356.

Vulpiani, G., S. Giangrande, and F. S. Marzano, 2009: Rainfall estimation from polarimetric s-band radar measurements: Validation of a neural network approach. *J. Applied Meteor. Climat.*, **48**, 2022–2036.

Vulpiani, G., M. Montopoli, L. Delli Passeri, A. G. Gioia, P. Giordano, and F. S. Marzano, 2012: On the use of dual-polarized C-band radar for operational rainfall retrieval in mountainous area. *J. Appl. Meteor. Climatol.*, **51**, 405–425.

Vulpiani, G., P. Tabary, J. Parent Du Chatelet, and F. S. Marzano, 2008: Comparison of advanced radar polarimetric techniques for operational attenuation correction at C band. *J. Atmos. Oceanic Technol.*, **25**, 1118–1135.

Wilson, J. W. and E. A. Brandes, 1979: Radar measurements of rainfall - a summary. *Bull. Amer. Meteor. Soc.*, **60**, 1048–1058.